Int. J. Electrochem. Sci., 8 **(2013)** 3197 - 3211

International Journal of
ELECTROCHEMICAL
SCIENCE
www.electrochemsci.org

Potentiometric Selective Recognition of Oxalic Acid Based on Molecularly Imprinted Polymer

Kiran Kumar Tadi, Ramani V. Motghare[*]

Department of Chemistry, Visvesvaraya National Institute of Technology, Nagpur-440011 (M.S), INDIA.
[*]E-mail: rkkawadkar@chm.vnit.ac.in

Received: 26 January 2013 / *Accepted:* 18 February 2013 / *Published:* 1 March 2013

This paper reports potentiometric determination of oxalic acid in spinach, using PVC-oxalic acid imprinted polymer coated graphite electrode. The intermolecular interactions between oxalic acid and acrylamide functional monomer and the number of moles of functional monomer that interact with one mole of template were studied using computational method based on density functional theory. Oxalic acid specific bulk polymer was obtained by the thermal initiated free radical co-polymerization of acrylamide and ethylene glycol dimethacrylate with oxalic acid as template and acetonitrile as porogen. After extraction of template, the binding parameters of molecularly imprinted polymer (MIP) and non-imprinted polymer (NIP) were compared by Langmuir- Freundlich (L-F) adsorption isotherms. After optimization of membrane composition, electrode coated with MIP-PVC membrane in dioctyl phthalate as plasticizer, exhibited super Nernstian response (36.83 ± 0.5 mV decade^{-1}) over a concentration range of 1.0×10^{-7} to 1.0×10^{-2} M, with a low detection limit of 1.2×10^{-7} M. The sensor showed good selectivity and was successfully applied for determination of oxalic acid in spinach and ground water samples.

Keywords: Computational approach; Molecularly imprinted polymer; Oxalic acid; Coated graphite electrode; Spinach analysis.

1. INTRODUCTION

Oxalic acid (OA) is widely distributed in various organisms, fungi, plants and animals. High levels of OA remove calcium from blood with severe disturbances in the activity of heart and neural system. It was found that OA may cause digestive tract irritation and kidney damage; therefore there is an increasing demand for its determination in biofluids [1, 2]. Wide range of colorimetric [3-5], enzymatic [6, 7] and chromatographic methods [8] were introduced to determine oxalic acid. However,

each method suffered from diverse disadvantages concerning cost ineffectiveness, insufficient selectivity, essential derivatization for sensitive detection and time consuming sample detection. Molecular imprinting technology provides synthetic receptors capable of recognizing traces of analytes in biofluids like blood, urine etc. It involves self assembled complexation of a substrate to functional monomers to form a pre-polymer complex, which is "locked-in" to place by co-polymerization with an excess of cross linking monomer [9]. Templates interact specifically with different functional monomers in different way to make covalent, non-covalent or semi-covalent complexes.

Oxalic acid is a simple hydrophilic molecule [log $K_{O/W}$ = -0.7] having high solubility in water. Therefore, MIP synthesis for this molecule is a difficult task. Uses of cyclodextrins [10], conversion of the hydrophilic template to hydrophobic one via alkyl chain attachment [11] are examples of MIP synthesis methods for water soluble compounds. Although, the synthesis of MIP looks quite easy, it is difficult to screen out the best functional monomer having more binding interactions with template. Combinatorial chemistry and molecular modeling are the most promising tools for the development of MIPs with enhanced recognition properties [12]. But the former suffers in the waste of chemicals and time. Computational modeling considerably reduces the tedious task of finding the best recipes for MIPs [13, 14]. Ab initio and semi-empirical methods were used to the design MIPs [15]. Dong et al. employed computational approach to screen monomers using the binding energy (ΔE) of the template theophylline [16] and monomers as a measure of their interaction. In the past few years, Density Functional Theory (DFT) has emerged as a cost effective computational method in which, the effects of electron correlation is included [17]. Modeling of functional monomer-template interactions and the resulting binding site performance evaluation is a successful approach towards more rational designing MIP technology [18].

In the present work, based on the computational studies oxalic acid imprinted polymer was synthesized under optimized conditions and electrode was fabricated using dioctyl phthalate as plasticizer. The fabricated PVC-MIP based sensor was successfully applied for determination of oxalic acid in ground water sample and spinach. To the best of our knowledge, this is the first report on potentiometric sensor for oxalic acid based on oxalic acid imprinted polymer, where oxalic acid imprinted polymer is prepared using computational data and is experimentally characterized and validated.

2. MATERIALS AND METHODS

2.1 Computational methods

The calculations of binding energies of template-monomer complex, involves several steps, mentioned as follows.

Building of models

The three-dimensional structure of the acrylamide (AA), oxalic acid (OA) template-monomer (OA-AA) complexes were built up with the aid of the AVOGADRO programme and pre-optimized by MMFF force field applying its implementation in the Avogadro programme.

Geometry optimization

The molecular geometries were optimized by using density functional theory at the B3LYP/6-31+G (d,p)// B3LYP/6-31G(d) level implemented in Gaussian 03 [20].

Frequency calculations

The optimizations were followed by computations of the harmonic vibrational frequencies to check local minima and no imaginary frequencies were obtained.

Energy calculations

The single point energy of each optimized conformations were calculated by using B3LYP/6-31+G(d,p) basis set. The ΔE values were calculated by using following equation.

$$\Delta E = E_{(template\text{-}monomer)} - (E_{template} + \sum E_{monomer})$$

The basis set superstition error (BSSE) substantially affects the calculated stabilization energies were corrected by means of the counterpoise method [21].

2.2 Experimental

2.2.1 Reagents and Apparatus

Acrylamide (ACR), dioctyl phthalate (DOP) and high molecular weight polyvinyl chloride (PVC) were purchased from Sigma Aldrich. Acetonitrile, Oxalic acid, Ethylene glycol dimethacrylate (EGDMA), Tetrahydrofuran (THF), hydrochloric acid are from Merck. Azobisisobutyronitrile (AIBN) was supplied by Across Organics. AIBN was recrystallized from methanol before use. All chemical were of analytical grade unless mentioned and all solutions are prepared in double distilled water. Standard sieve of BSS number 200 (sieve size 75 microns) was used to get fine MIP/NIP particles.

All potentials were measured on digital Hioki 3244-60 vs a Systronics saturated calomel reference electrode (SCE) at 25 $\pm$ 0.1^0C. Shimazdu model IRaffinity FTIR spectrometer was used for recording IR spectra of MIP, NIP and acrylamide functional monomer. A Shimazdu model UV-1800 spectrophotometer equipped with quartz cell of 1 cm path length was used for recording absorbance spectra. Toshniwal pH meter was used for measuring pH of the eluents.

2.2.2 Preparation of Oxalic acid imprinted polymer and non-imprinted polymer

The template (OA) 0.25 mmol, functional monomer (acrylamide) 1.0 mmol and 5 ml of acetonitrile were placed in 15ml glass vial. The contents were shaked well to ensure formation of pre-polymerization complex. Subsequently, EGDMA (cross linker) 10 mmoles and initiator AIBN 0.15mmol were added. The mixture was purged with nitrogen for 10 minutes to create inert atmosphere. The vial was completely sealed and kept in water bath at 55°C for 12 hours to complete polymerization reaction.

The control or non-imprinted polymer (NIP) was also prepared in the same manner but without addition of template. The glass vial was broken and the resultant rigid bulk products were washed with

water to remove unreacted precursors, dried, crushed and ground into powder using mortar and pestle, sieved through 75 micron sieve to get fine particles. The polymer was washed with double distilled water to elute the template and then complete elution of template was confirmed from pH of the eluent as well as by UV/VIS spectrophotometer. The particles were dried under vacuum at 50°C overnight and then used for further studies.

2.2.3 Binding studies

The binding capacity of MIP and NIP were determined by batch rebinding experiments. In the binding assay, 0.1 gm of MIP or NIP was added to 20ml aqueous solution of oxalic acid of different concentrations and stirred for 5 hours at 25°C. The polymer particles were filtered off and filtrate was analyzed for oxalic acid by UV/VIS spectrophotometer. The quantity of bound oxalic acid was determined by subtracting the equilibrium amount of template from initial quantity of template. The experimental binding data were fitted to the Langmuir-Freundlich (L-F) adsorption models.

2.2.4 Electrode fabrication

General procedure for preparation of PVC membrane was adopted from previous literature [22, 23]. 60 mg of PVC were dissolved in 2.5 ml THF. 40 mg oxalic acid imprinted polymer particles or non-imprinted particles were dispersed in 0.2 ml DOP and were mixed to the above solution and homogenized. Graphite electrodes of 3mm diameter and 10 mm length were polished with alumina slurry on a polishing cloth, sonicated for 5 minutes in distilled water and dried in air. The electrode was coated with the above homogenized solution and dried for 5 minutes to form a uniform film. The process was repeated 2-3 times to form a plastic membrane of thickness ~0.3 mm and finally dried for 3 hours. The sensor was conditioned in 25 ml of 10^{-3} M oxalic acid for 15 hours.

The following cell assembly was used for measurements of all EMF's

SCE// sample solution/ MIP based membrane/graphite electrode

The coated electrode containing MIP was used as the working electrode in conjunction with a saturated calomel electrode.

2.2.5 Spinach sample preparation

For spinach extract, 10 g sample was cut into small pieces with a razor blade and pounded into paste in a mortar with a pestle, and then diluted to 1 liter with water in a volumetric flask. The suspension was centrifuged at 4000 rpm for 5 minutes and the supernatant filtered through A-1 filter paper. 50 ml of resultant extract was spiked with oxalic acid of different concentrations and analyzed using above fabricated electrode by analytical procedure as mentioned in section 2.2.4

3. RESULTS AND DISCUSSION

3.1 Computational studies

3.1.1 Selection of functional monomer for synthesis of OA-imprinted polymer.

Table 1, shows the binding energies of complexes formed between oxalic acid and different functional monomers.

From the values in table 1, it is evident that among different acidic, basic and neutral functional monomers, acrylamide forms the most stable complex with oxalic acid. This was also emphasized by Klaus Mosbach, when the template has hydrogen bonding functional groups, acrylamide serves as the best functional monomer in polar solvents [24].

Table 1. Interaction energies of pre-polymer complex between template and the functional monomers

Molecules	Interaction energy ΔE (kcal/mol)
Oxalic acid-Acrylamide	-14.307
Oxalic acid-acrylic acid	-12.145
Oxalic acid-Allyl amine	-10.667
Oxalic acid-4 Vinylpyridine	-2.6138
Oxalic acid-methacrylic acid	-9.756
Oxalic acid-methyl methacrylic acid	-7.906

3.1.2 Optimization of template: functional monomer ratio

Table2. Interaction energies for 1/1 to 1/4 template-monomer ratios

Molecules	Energy (Hartrees/Particle)	Interaction energy ΔE (kcal/mol)
Oxalic acid	-378.3508	---
Acrylamide (AA)	-247.3193	---
OA-AA	-625.6929	-14.307
OA-$(AA)_2$	-873.0268	-23.120
OA-$(AA)_3$	1120.3651	-35.328
OA-$(AA)_4$	-1367.6931	-40.806

If excess moles of functional monomer were used, only specific number of moles reacts with template and rest which remain as excess leads to non-specific binding [25] and hence decreases the binding capacity. So, the numbers of moles of functional monomer that interacts with one mole of template were optimized. From the results in table 2, it can be concluded that order of the molecular interaction is as follows: OA-AA (1:4) > OA-AA (1:3) > OA-AA (1:2) > OA-AA (1:1). These results show that the complex in 1:4 ratio has highest binding energy and thus leads to the formation of the most stable complex.

Four possible forms [cis-OA-AA (1-2) and trans-OA-AA (1-2)] were studied after the optimization of oxalic acid to acrylamide mole ratio. It could be observed from the table 3 that *trans*-OA-AA (2) complex with a binding energy of -46.74 Kcal/mol is the most stable conformation.

Table 3. Interaction energies (ΔE) for Cis Oxalic acid-AA (1-2) and Trans Oxalic acid-AA(1-2)

Compound	Energy (Hartrees/Particle)	Interaction energy ΔE (kcal/mol)
Cis-OA-AA (1)	-1367.688	-38.140
Cis-OA-AA (2)	-1367.690	-39.206
Trans-OA-AA (1)	-1367.689	-33.747
Trans-OA-AA (2)	-1367.702	-46.749

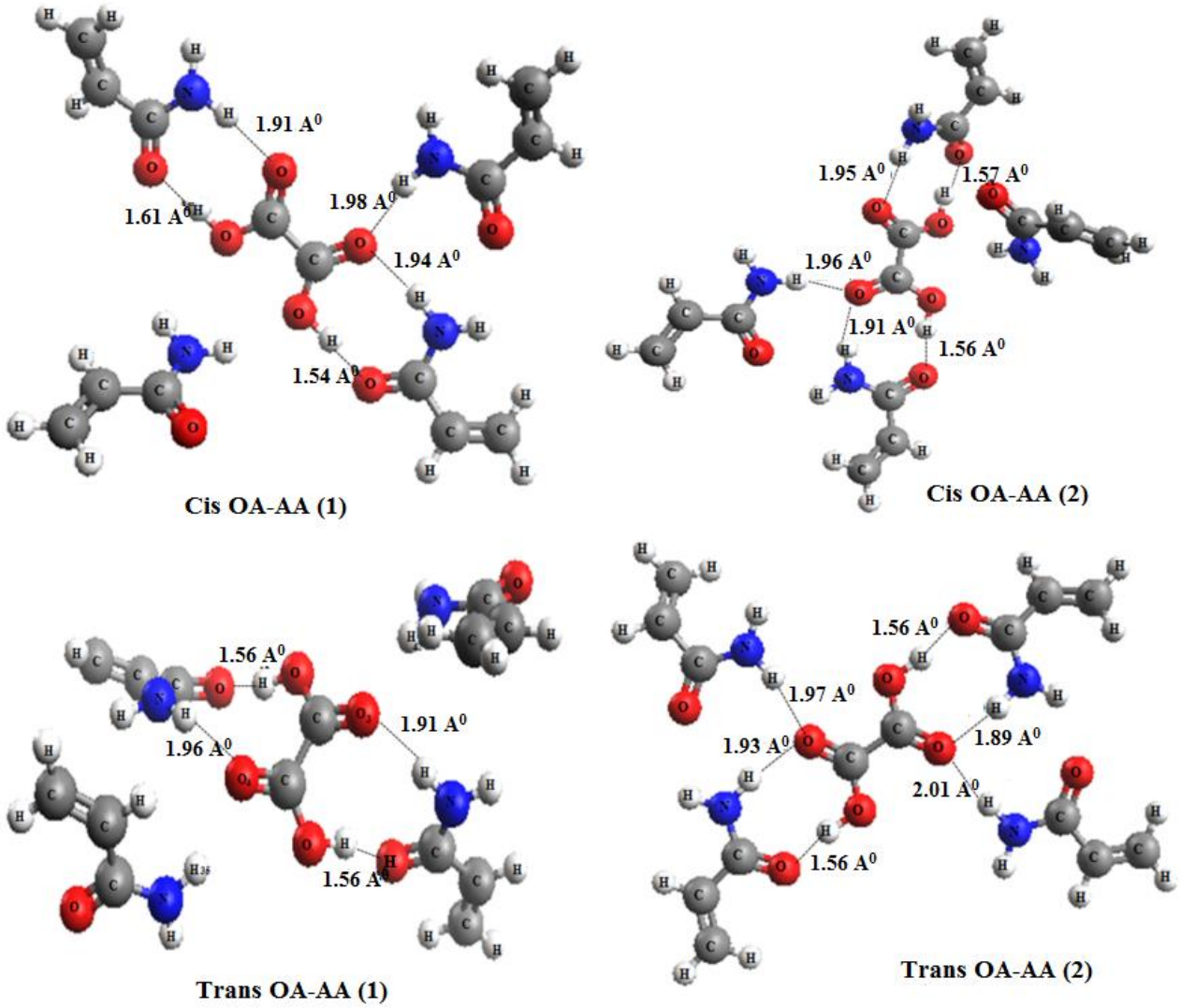

Figure 1. Optimized structures showing hydrogen bonding for the four complexes, cis-OA-AA (1- 2) and trans-OA-AA (1-2) (Å)

In non-covalent imprinting protocol hydrogen bonding plays an important role in stabilizing the pre-polymerization complex [26]. The structures of all the four studied complexes of 1:4 ratios are shown in Figure 1. It is evident from the structures that cis-OA-AA (1-2) interacts with three acrylamide molecules and one remains free but trans-OA-AA(2) interacts with four functional monomer molecules. In Trans-OA-AA(1), oxalic was found to have hydrogen bonding with two acrylamide molecules and weak (distance between H_{35}---O_4 is 2.06 Å and for H_{42}---O_3 is 2.09 Å) interactions with other two acrylamide molecules. This reveals the formation of Trans-OA-AA (1) complex with four acrylamide molecules.

3.2 Study of synthesized polymers

3.2.1 Characterization by FTIR spectra

The FT-IR spectra of NIP, oxalic acid imprinted polymer and functional monomer were recorded using KBr pellet method. Spectral differences between NIP, MIP and functional monomer are shown in figure 2. Both MIP and NIP have similar IR spectra indicating similarity in backbone structure. But the interaction between template and monomer gave changeable bands in MIP spectrum, which shows a broad OH stretching band due to hydrogen bonded amide (N-H) and hydroxyl group (OH) at 3150- 3350 cm^{-1}.

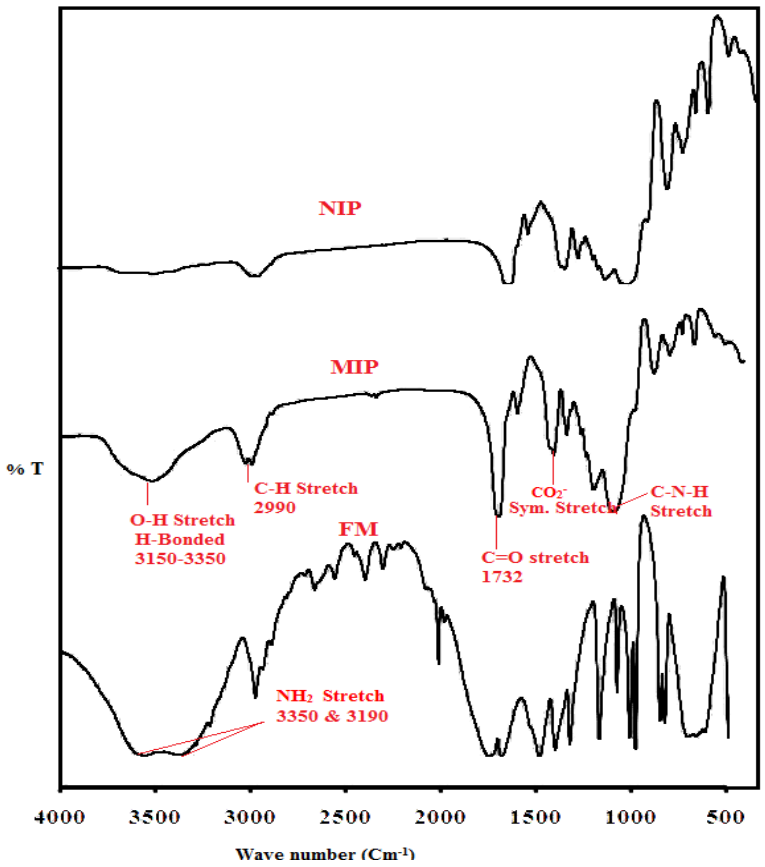

Figure 2. IR Spectra of MIP, NIP and acrylamide

CH stretching at 2956 cm^{-1} and 2989 cm^{-1}, while the CH stretching in spectrum of acrylamide was observed at 2812 cm^{-1}. No band was observed in this region due to absence of interactions between acrylamide and oxalic acid in NIP. C=O stretching vibrations were found at 1732 cm^{-1} which shows a very strong carbonyl group of amide. A band at 1456 cm^{-1} corresponds to symmetric stretching of carboxylate ion and at 1159 cm^{-1} results from the interaction between N-H bending and C-N stretching.

3.2.2 Adsorption Isotherm study

All imprinted polymers cannot be modeled using solely Freundlich or Langmuir isotherms. The Langmuir isotherm best models the saturation behavior of MIP, usually in the high concentration region whereas the Freundlich isotherm is limited to the lower sub-saturation concentration region of the binding isotherms. These isotherms require hybrid heterogeneous binding models that can span both saturation and sub-saturation regions [27]. Along these lines we have applied the Langmuir-Freundlich (LF) isotherm (Eq.1) to characterize MIPs. The LF model describes the relationship between equilibrium concentration of bound (B) and free (C) analyte to characterize MIPs (Fig. 3).

$$B = \frac{N\, a\, C^{m}}{(1 + a\, C^{m})} \qquad (1)$$

Where 'B' (mmol g^{-1}) is the amount of adsorbed analyte per unit weight of polymer, C (mmol L^{-1}) is the concentration of analyte in the distribution of binding sites of varying binding strengths present in the polymer and 'm' is the heterogeneity index with values between zero to one and N is the total number of binding sites. The equation 1 was used to fit the adsorption isotherm by a non-linear least square-fitting program as shown in figure 3, which yielded fitting parameters 'a', 'm', 'N' and K_0 (= $a^{1/m}$) and the values given in table 4.

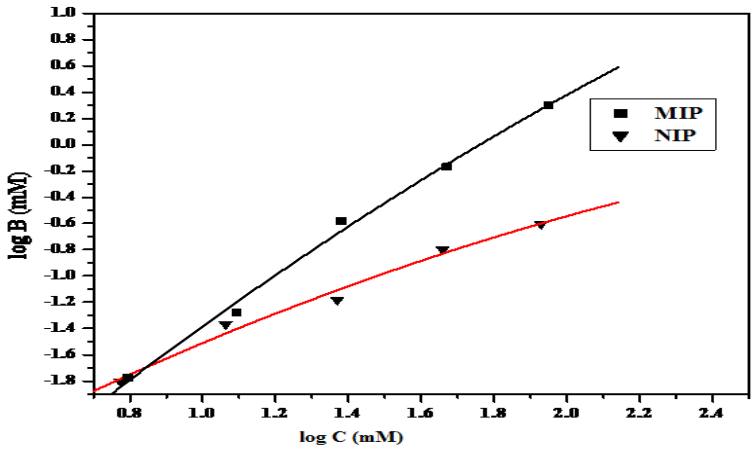

Figure 3. Langmuir-Freundlich (L-F) adsorption Isotherm for Oxalic acid MIP and NIP

The values obtained from Langmuir-Freundlich model indicates that MIP studied possess more number of binding sites (N) than the corresponding NIP. Similarly affinity distribution of binding sites 'a' in MIP is greater than in NIP due to definite shape and selectivity of the polymer and it is evident that this system has a distribution of binding sites of varying binding affinity values of 'm' between 0 and 1 confirm the existence of heterogeneity which is dependent on the differences in the chemical groups distribution, and the shape of the imprinted pockets. From the binding parameters generated; it was observed that MIP has appreciable number of binding sites.

Table 4. Fitting coefficients for the Langmuir-Freundlich (L-F) models of the MIP

Langmuir-Freundlich (L-F)	MIP	NIP
N (mmol g^{-1})	32.546	10.015
a (M^{-1})	0.156	0.129
m	0.9452	0.50
R^2	0.9867	0.9460

3.3 Optimization of Membrane composition

In any chemical sensor, a chemical or physical signal generated upon binding of analyte to the recognition element or receptor, which is then translated into a quantifiable output signal by the transducer. The receptor function is fulfilled by a thin layer of MIP-PVC membrane. The main function of receptor in a chemical or bio-sensor is to respond selectively to particular substances or to a group of substances [28]. The linear range of potentiometric sensor can be increased by incorporating suitable plasticizer so that it enhances mobility of target analytes. In our experiment, dioctyl phthalate (DOP) was selected as a plasticizer due to its low dielectric constant (ε =5.0). Since the weight of MIP particles determine the number of binding sites available for selective rebinding of analyte, the ratio of MIP to PVC was found to be a key factor in sensor performance.

Table 5. Effect of membrane composition on MIP-based oxalate anion electrode

Membrane No.	Wt. of MIP (gm)	Wt. of PVC (gm)	DOP (mL)	Linearity range	Slope (mV/decade)
1	0.01	0.06	0.2	10^{-7} -10^{-5}	4.32
				10^{-5} -10^{-2}	41.90
2	0.02	0.06	0.2	10^{-7} -10^{-5}	7.42
				10^{-5} -10^{-2}	30.35
3	0.03	0.06	0.2	10^{-7} -10^{-2}	20.22
4*	0.04	0.06	0.2	10^{-7} -10^{-2}	36.83
5	0.05	0.06	0.2	10^{-7} -10^{-2}	50.59
6	0.035	0.06	0.2	10^{-7} -10^{-2}	34.48
7	0.045	0.06	0.2	10^{-7} -10^{-2}	28.86

* optimum composition

The effect of change in the ratio of MIP to PVC in the membrane with 0.2 ml of DOP was investigated and the results are shown in table 5. The sensitivity of electrode response increases with increase in MIP content till a value of 40 mg and MIP/PVC ratio up to 0.83 is reached. Although, the highest sensitivity was observed for 50 mg MIP and 60 mg PVC combination, but showed high standard deviation. Hence, the electrode made from membrane containing 40 mg MIP and 60 mg PVC was found to be optimum one in the development of this sensor (membrane no. 4, table 5).

3.4 Evaluation of fabricated electrodes

3.4.1 Calibration curve

The potential response of MIP and NIP sensors fabricated under the optimal conditions were studied. As seen from figure 4, the potentials are increasing in positive direction with increasing oxalic acid concentration.

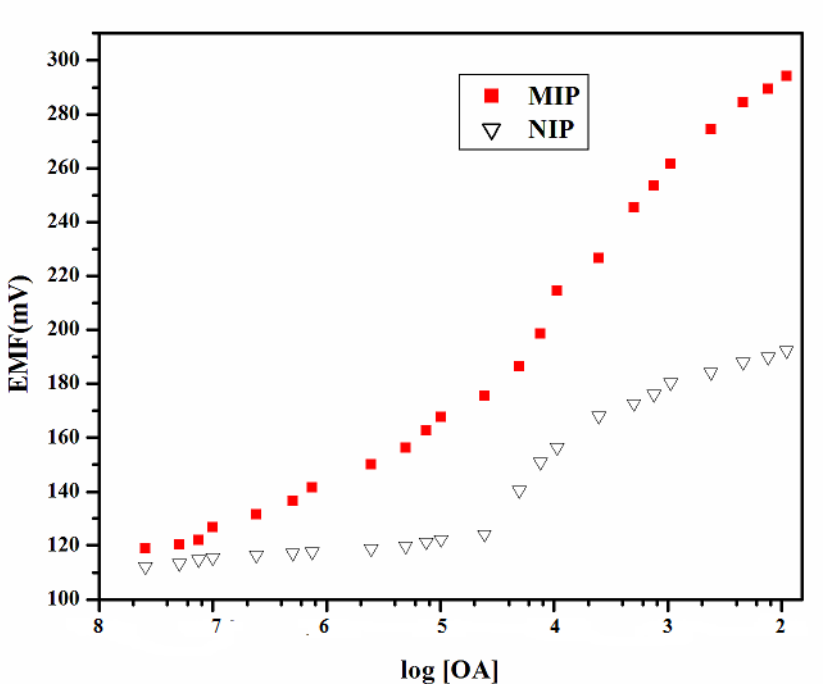

Figure 4. Calibration plot for the oxalate anion selective electrode with optimized membrane composition based on MIP and NIP particles

The same kind of behavior was reported in the case of methylphosphonic acid imprinted polymer based potentiometric sensor by K.P Prathish et al. [22] and nitrate ion-selective sensor by Bianting Sun et al. [29]. This may be due to co-extraction equilibrium process, where the anion (oxalate ion) is extracted by the membrane [30, 31] as shown in scheme 1.

$$Ox^{-}(\text{aqueous}) + H^{+}(\text{aqueous}) + M(\text{organic phase}) \rightleftharpoons Ox\,M^{-}(\text{organic phase}) + H^{+}$$

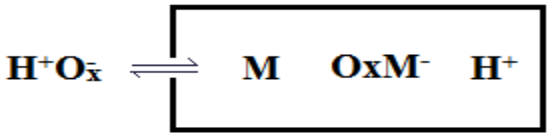

Scheme 1. Schematic representation of MIP (neutral carrier) mechanism

The box designate the organic phase, Ox^- and H^+ the charged sites of the analyte and M the molecularly imprinted polymer.

The calibration plot obtained for the MIP based sensors offer a working range of 1.0×10^{-7} to 1.0×10^{-2} M with a super Nerstian slope of 36.83 ± 0.5 mV/decade. The cavities present in oxalic acid imprinted polymer, are attributed to the specific response of MIP-PVC electrode. In contrast NIP based sensor is showing linearity in the range 2.5×10^{-5} M to 1.0×10^{-3} M which may be due to amide groups on the surface of polymer having non-specific interactions with oxalate anion.

The limit of detection was determined from the intersection of two extrapolated segments [32] on the calibration graph as 1.2×10^{-7} M.

3.4.2 Dynamic response time & reversibility

Dynamic response time is an important characteristic for an ion-selective electrode. For this purpose, practical response time was recorded by changing oxalic acid concentrations from 1.0×10^{-6} M to 5.0×10^{-4} M. The measurement sequence was from lower (1.0×10^{-6} M) to higher (5.0×10^{-4} M) concentrations.

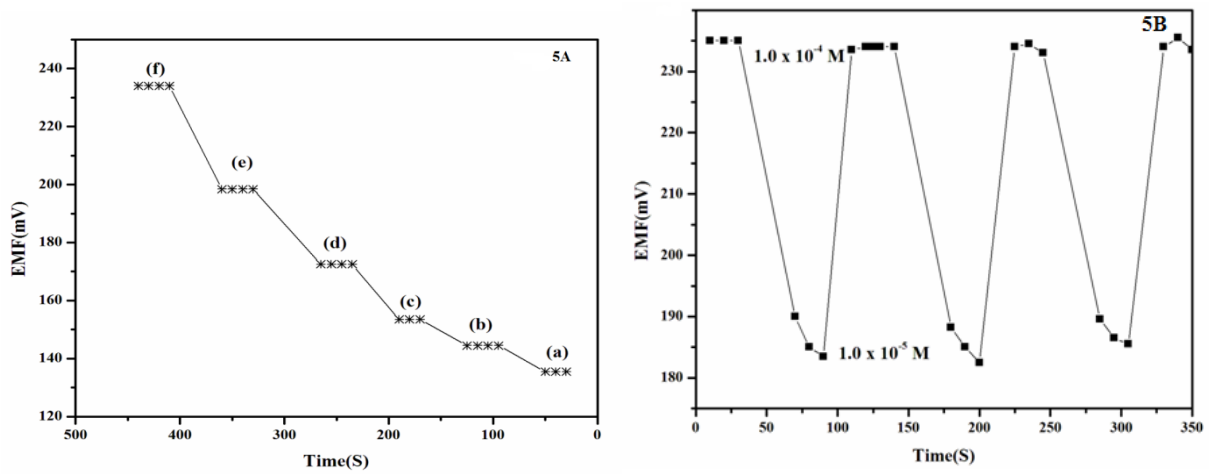

Figure 5. (A) Dynamic response time of electrode for one change in concentration of oxalic acid (a)1.0×10^{-6}M, (b) 5.0×10^{-6}M, (c) 1.0×10^{-5} M, (d) 5.0×10^{-5}M, (e) 1.0×10^{-4} M and (f) 5×10^{-4} M **(B)** Reversibility of oxalic acid selective Electrode in several high-to-low sample cycles

Figure 5A shows actual potential vs. time traces. It can be seen from the figure that the electrode reaches equilibrium response in 60 seconds.

Reversibility of the electrode was evaluated by performing measurements in sequence of high-to-low sample concentrations and the results are shown in figure 5B. Here, it is seen that the potentiometric response of the sensor is reversible, although the time needed to reach equilibrium values are longer than that for the high-to-low sample concentrations.

3.4.3 Effect of pH

Effect of oxalic acid test solution (10^{-5} and 10^{-3} M) pH on the electrode potential was investigated by changing pH (by adding small volumes of HCl/ NaOH), shown as a plot of EMF vs. pH (Fig. 6). As seen from figure 6, within the pH range 4 to 9, the electrode potential is practically independent of pH, and thus, this range will be taken as the working pH range for the proposed sensor. The deviation in electrode potential at pH < 4 may be due to the H^+ ions and at pH > 9, OH^- ions compete with oxalate ions. The pH dependence is very similar to that reported by Bianting et al. [29] and Dong et al. [33] although the sensing anions are different.

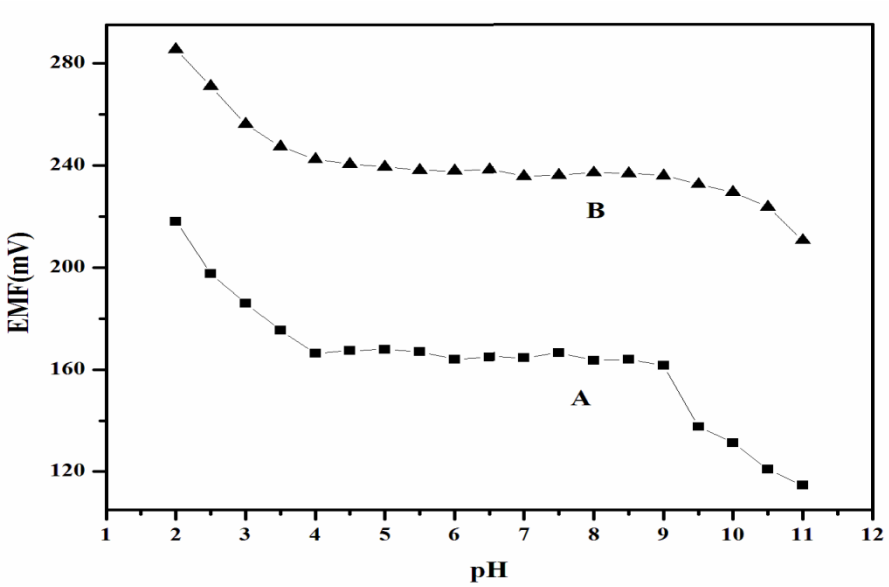

Figure 6. Effect of test solution pH on the potential response of the oxalic acid selective sensor at (A) 1.0×10^{-5} M and (B) 1.0×10^{-4} M

3.4.4 Selectivity of sensor

Halides and several other common anions including structural analogues of oxalic acid were tested using MIP and NIP based oxalic acid sensors in order to study the degree of interference from each. The potentiometric response results were obtained by using fixed interferent method [34]. The selectivity coefficients of MIP and NIP based sensor electrodes were determined by mixing 1×10^{-3} M

interferent with various oxalic acid standard solutions of 10^{-7} to 10^{-2} M and the results were shown in table 6. It was found, that selectivity coefficients obtained for the examined anions shows that most of these compounds do not disturb functioning of the oxalic acid selective electrode significantly.

Among halides (F, Cl, Br and I), the values of $K^{Pot}_{OA,Cl-}$ of MIP is closer to the value of NIP electrode where as good differences between MIP and NIP were observed in case of iodide. This may be due to the differences in higher and lower electro negativities of chloride and iodide ions respectively, which enhances formation of hydrogen bonding with amide groups present in NIP. Quite interestingly, oxalic acid sensor based on MIP shows good selectivity even in case of template structural analogues especially for maleic acid.

Table 6. Selectivity coefficient values of proposed electrode based on the MIP and NIP particles.

Interferent J	MIP	NIP	Interferent J	MIP	NIP
Fluoride	5.0×10^{-4}	1.0×10^{-3}	Sulphate	9.0×10^{-6}	1.2×10^{-5}
Chloride	5.5×10^{-4}	2.1×10^{-4}	Tartarate	2.3×10^{-5}	5.0×10^{-4}
Bromide	8.2×10^{-4}	1.0×10^{-4}	Maleate	6.0×10^{-4}	4.0×10^{-4}
Iodide	5.5×10^{-6}	8.5×10^{-4}	Urea	8.5×10^{-5}	1.5×10^{-5}
Bicarbonate	7.0×10^{-5}	9.5×10^{-4}	Phosphate	7.5×10^{-5}	1.5×10^{-4}
Formate	6.2×10^{-4}	9.0×10^{-5}			
Acetate	5.0×10^{-5}	1.5×10^{-4}			
Nitrate	9.0×10^{-5}	1.8×10^{-4}			

3.4.5 Analytical application

Table 7. Analysis of oxalic acid in real samples

Sample	Concentrations of selected interferent in mixture spiked to the samples (mol.L^{-1})[a]	Oxalic acid Added (10^{-6} mol. L^{-1})	Oxalic acid Found[b] (10^{-6} mol. L^{-1})	Recovery (%)
Spinach	-	1.0	0.962	96.2
	10^{-7}	1.0	0.955	95.5
	10^{-6}	1.0	0.957	95.7
	10^{-5}	1.0	0.956	95.6
Ground water	-	1.0	0.960	96.0
	10^{-7}	1.0	0.943	94.3
	10^{-6}	1.0	0.939	93.9
	10^{-5}	1.0	0.929	92.9

a mixture of maleic acid and tartaric acid; b average of three determinations

To investigate applicability of the fabricated sensor to real samples, the membrane sensor was used to determine oxalic acid in water extracts from spinach and ground water.

It was successfully applied to spinach and ground water samples, as it is clear from the selectivity studies that several interferants co-exist in real samples but they don't have any deleterious effect on performance of potentiometric membrane sensor. Spinach and ground water samples were analyzed by spiking known amounts of oxalic acid and varying concentrations of interferent mixtures. The results thus obtained are shown in table 7**.** The recovery obtained in the range 95-96% for spinach, where as 92-94% for ground water. This may be due to the organic interferants from spinach causing less effect than inorganic interferants from ground water on the performance of membrane sensor.

4. CONCLUSIONS

From quantum chemical calculations, it was found that 1:4 template monomer ratio is the best configuration. More favoured interactions were found between trans-oxalic acid and acrylamide. The trans-OA-AA-2 was the most stable complex with binding energy - 46.749 Kcal/Mol. The oxalic acid MIP synthesized by bulk polymerization shows better binding capacity than non-imprinted polymer.

The fabricated potentiometric sensor shows a super Nernstian over a range of concentration 1.0 $\times 10^{-7}$ to 1.0 $\times 10^{-2}$ M, with a detection limit 1.2 $\times 10^{-7}$ mol L^{-1} compared to corresponding non-imprinted polymer based potentiometric sensor. The interferants co-exist in real samples but do not have any deleterious effect on the sensor performance. Moreover, the sensor shows fast response time and selectivity over a large number of anions. The obtained sensor showed suitable analytical performance for the determination of oxalic acid in spinach and ground water samples.

ACKNOWLEDGEMENTS
We are grateful to Dr. R.M.Patrikar, Electronics and Communication Engineering Department, VNIT, Nagpur for giving opportunity to work on Gaussian 03 Software.

References

1. Health Council of the Netherlands, (2004). Health-based reassessment administrative exposure limits: oxalic acid. 2000/15OSH/106.
2. R. Menache, *Clin. Chem.*, 20 (1974) 1444.
3. P.M Zarembski and A. Hodgkinson, *Analyst*, 87 (1962) 698.
4. Z.L Jiang, M.X Zhao, M and L. Lin-Xiu, *Anal. Chim. Acta*, 320 (1996) 139.
5. A.A. Ensafi and M Emadi, (2004). *Anal.l Lett.*, 37 (2004), 321.
6. G. Kohlbecker and M. Butz, *J. Clin. Chem. Clin. Bio.*, 19 (1981), 1103.
7. R. Haeckel and F.R Heinz and *Z. Klin. Chem. Klin. Biochem.*, 8 (1970), 480.
8. M.H Khaskhali, M.I Bhanger and F.D Khand, *J. Chromatogr. B*, 675 (1996), 147.
9. Mingdi Yan, Olof Ramstrom, *Molecularly imprinted materials*, Marcel Dekker, New York (2005).
10. H. Asanuma, T. Akiyama, K. Kajiya, T. Hishiya and M Komiyama, *Anal. Chim. Acta*, 435 (2001), 25.
11. P. Manesiotis, A.J Hall, J. Courtois, K. Irgum and B. Sellergren, *Angew Chem. Int. Edit*, 44 (2005), 3902.

12. C.F.V Nostrum, *Drug Disc. Today*, 2 (2005), 119.
13. M.S Khan, S. Prateek, S. Wate and R.J Krupadam, *J. Mol. Model.*, 18 (2012), 1969.
14. Nicholls, A. Ian, S. Hakan, Andersson, Christy Charlton, John O'Mahony and K.R. Johan, *Biosens. Bioelectron.*, 25 (2009), 543.
15. M. Azenha, P. Kathirvel, P. Nogueira and A. Fernando-Silva, *Biosens. Bioelectron.*, 23 (2008), 1843.
16. W. Dong, M. Yan, M. Zhang, Z. Liu and Y. Lin, *Anal. Chim. Acta.*, 542 (2005), 186.
17. S. Riahi, F. Edris-Tabrizi, M. Javanbakht, M.R Ganajali and P. Narouzi, *J. Mol. Model.*, 15 (2009), 829.
18. I. Chianella, S.A Piletsky, I.E. Tothill, B. Chen and A.P.F Turner, *Biosens. Bioelectron.*, 18 (2003), 119.
19. R. Chitra, A. Das, R.R. Choudary, R. Ramanadham and R. Chidamabaram, *J. Physics*, 63 (2004), 263.
20. Gaussian 03 2004 Revision C.02, Gaussian, Inc.: Wallingford, CT, USA.
21. D.W. Schwenke and D.G. Truhlar, *J. Chem. Physics*,82 (1985), 2418.
22. K. Prasad, K.P Prathish, J.M Gladis, G.R. K Naidu and T. Prasada Rao, *Sensor Actuat. B-Chem*, 123 (2007), 65.
23. M.R Ganjali, F. Aboufazeli, S. Riahi, R. Dinarvand, P. Norouz, M.H Ghasemi, R.K. Anbuhi and S. Meftah, Int. *J. Electrochem. Sci.*, 4 (2009), 1138.
24. Cong Yu and K. Mosbach, *J. Org. Chem.*, 62 (1997), 4057.
25. M. Komiyama, T. Takeuchi, T. Mukawa and H. Asanuma, *Molecular Imprinting; from fundamentals to applications*, Wiley-VCH (2003).
26. K. Karim, F. Breton and R. Rouillon, *Adv. Drug Deliver. Rev.*, 57 (2005), 1795.
27. R.J. Umpebly, C.B Sarah, C. Yizhao, N. Ripal, Shah, Shimzu and D. Ken, *Anal. Chem.*, 73 (2001), 4584.
28. P. Grundler, *Chemical sensors-An Introduction to for Scientists and Engineers,* Springer-Verlag Berlin Heidelberg (2007).
29. B. Sun and P.G Fitch, *Electroanal.*, 9 (1996), 494.
30. E. Bakker, E. Malinowska, R. Schiller and M.E Meyerhoff, *Talanta*, 41 (1994), 881.
31. P. Buhlmann, E. Pretsch and E. Bakker, *Chem. Rev.*, 97 (1997), 3083.
32. Analytical Methods Committee, *Analyst*, 112 (1987), 199.
33. S. Dong, Z. Sun and Z. Lu, *Analyst*, 113 (1988), 1525.
34. R.P Buck and E. Linder, *Pure Appl Chem*, 66 (1994), 2527.